Cancer Cell, Volume *28*

Supplemental Information

NEMO Prevents Steatohepatitis and Hepatocellular Carcinoma by Inhibiting RIPK1 Kinase Activity-Mediated Hepatocyte Apoptosis

Vangelis Kondylis, Apostolos Polykratis, Hanno Ehlken, Laura Ochoa-Callejero, Beate Katharina Straub, Santosh Krishna-Subramanian, Trieu-My Van, Harald-Morten Curth, Nicole Heise, Falk Weih, Ulf Klein, Peter Schirmacher, Michelle Kelliher, and Manolis Pasparakis

Supplemental Data

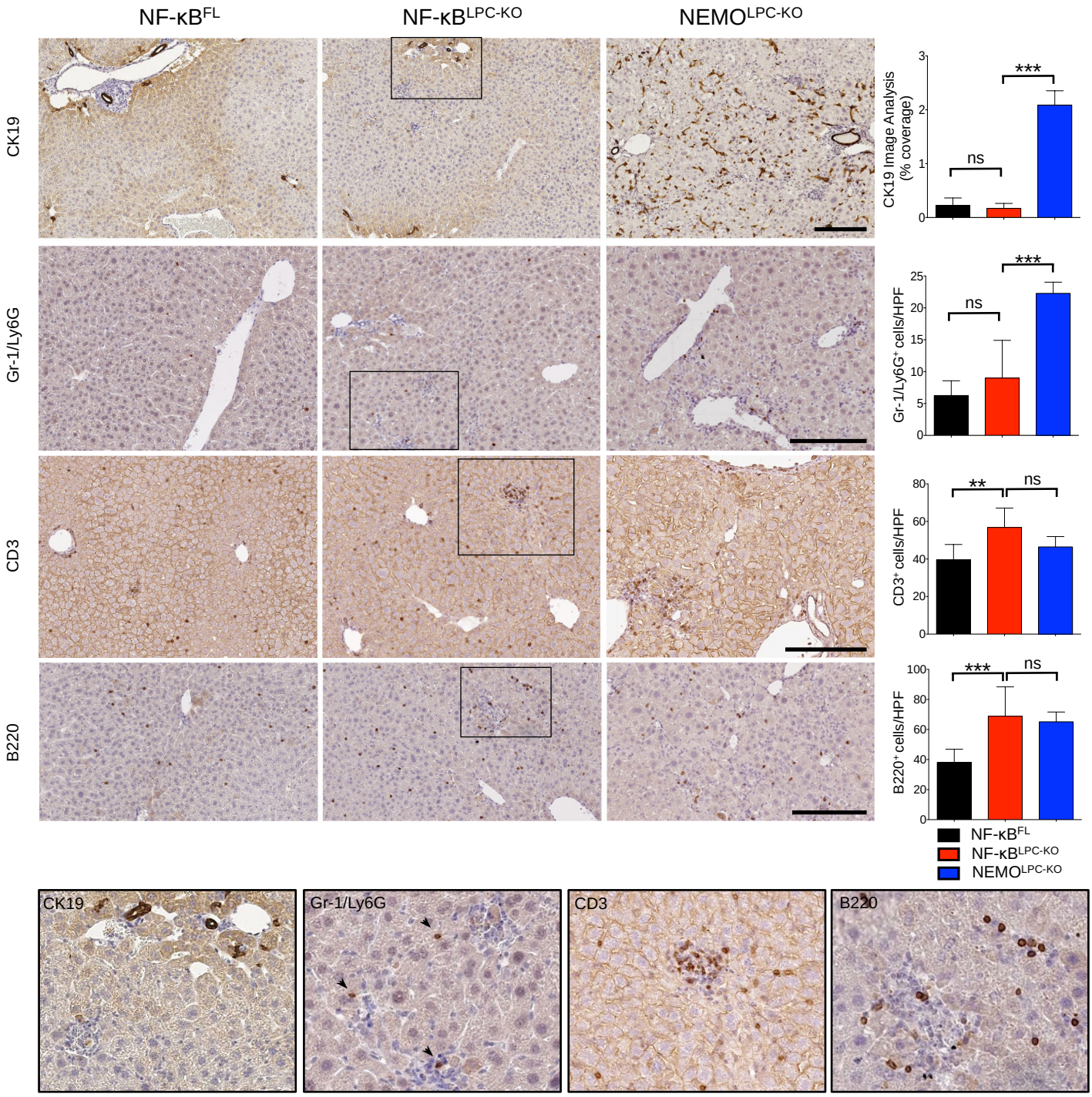

Figure S1, related to Figure 1: NF-κB^{LPC-KO} mice exhibit mild inflammatory cell infiltration but not activation of hepatic progenitor cells. Immunohistochemistry for hepatic progenitor cell marker (CK19), granulocyte marker (Ly6G), T cell marker (CD3), and B cell marker (B220), on paraffin-embedded liver sections from 8-week-old mice with the indicated genotypes. Higher magnifications of the boxed areas are shown below and graphs depict quantification of indicated parameters (mean ±SD, n=3-5 mice per genotype). Scale bars: 200 μm.

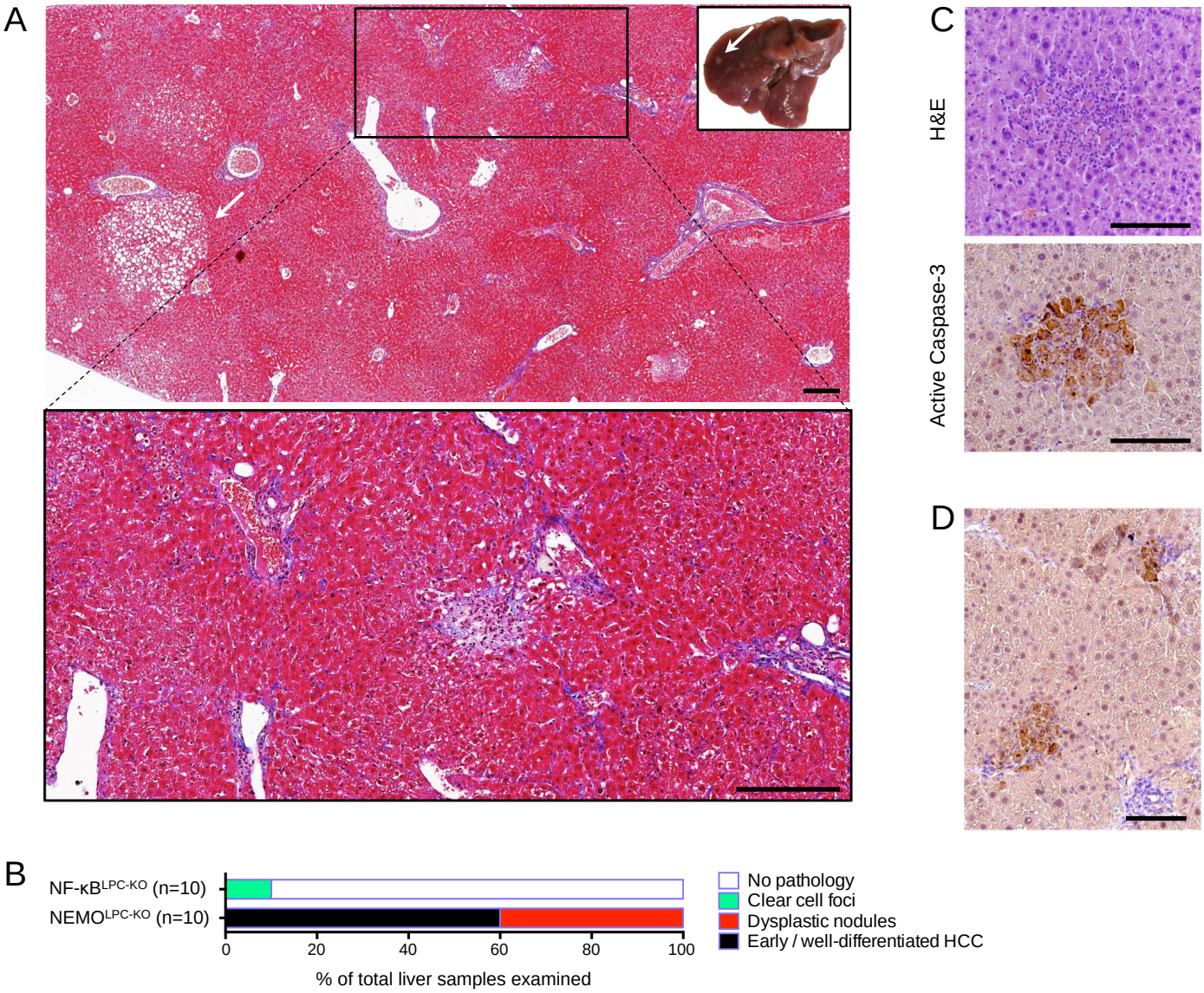

Figure S2, related to Figure 2: LPC-specific NF-κB deficiency alone is not sufficient to promote HCC development as observed in NEMO^{LPC-KO} mice. (A) Masson's trichrome staining showing extensive collagen deposition (in blue) and steatotic nodules (marked by white arrow) in the liver of an NF-κB^{LPC-KO} mouse with macroscopically visible very small nodules. The appearance of the examined liver is shown in the inset, and a higher magnification of the boxed area is shown. (B) Histopathological evaluation of HCC development in one-year-old mice with the indicated genotypes. Each color bar represents the % of livers per genotype in which the indicated stage was identified as the most advanced disease stage. n is indicated. Four control floxed samples per mouse line were examined without showing any pathological findings (not shown). (C) H&E and active caspase-3 staining of the same liver area on serial sections from a 52-week-old NF-κB^{LPC-KO} mouse. (D) Examples of focal apoptosis on a liver section from a 52-week-old NF-κB^{LPC-KO} mouse after immunostaining for active caspase-3. Scale bars: (A) 200 µm; (C,D) 100 µm.

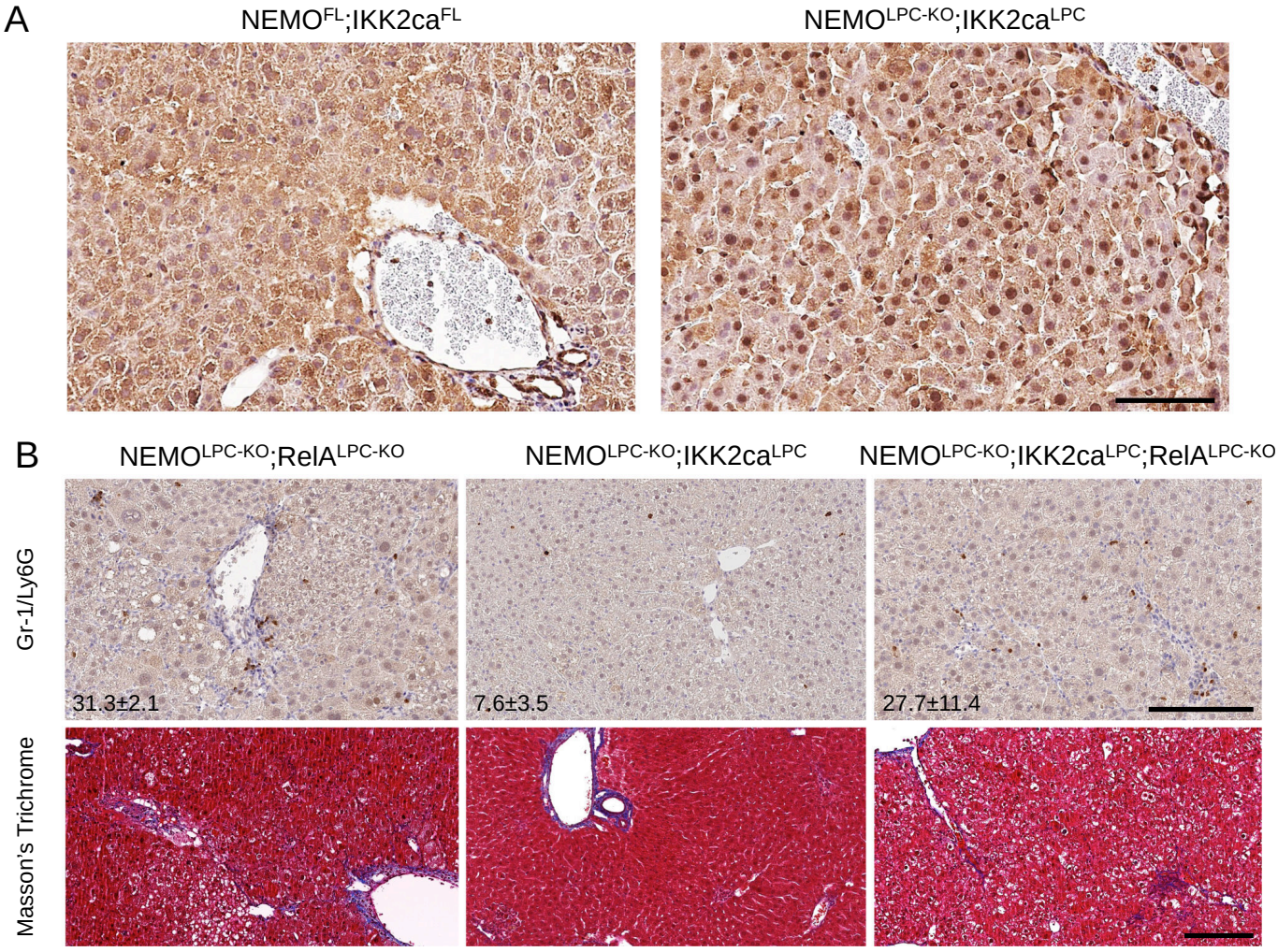

Figure S3, related to Figure 3: IKK2ca expression prevents the development of chronic liver pathology in NEMO^{LPC-KO} mice in an NF-κB-dependent way. (A) RelA/p65 immunostaining performed on paraffin-embedded liver sections. (B) Immunohistochemistry for granulocyte marker (Gr-1/Ly6G), and Masson´s trichrome staining on paraffin-embedded liver sections from 8-week-old mice with the indicated genotypes. Quantification of granulocytes (number of cells/HPF) is shown at the bottom left of each panel (mean ±SD, n=3-5 mice per genotype). Scale bars: 200 µm.

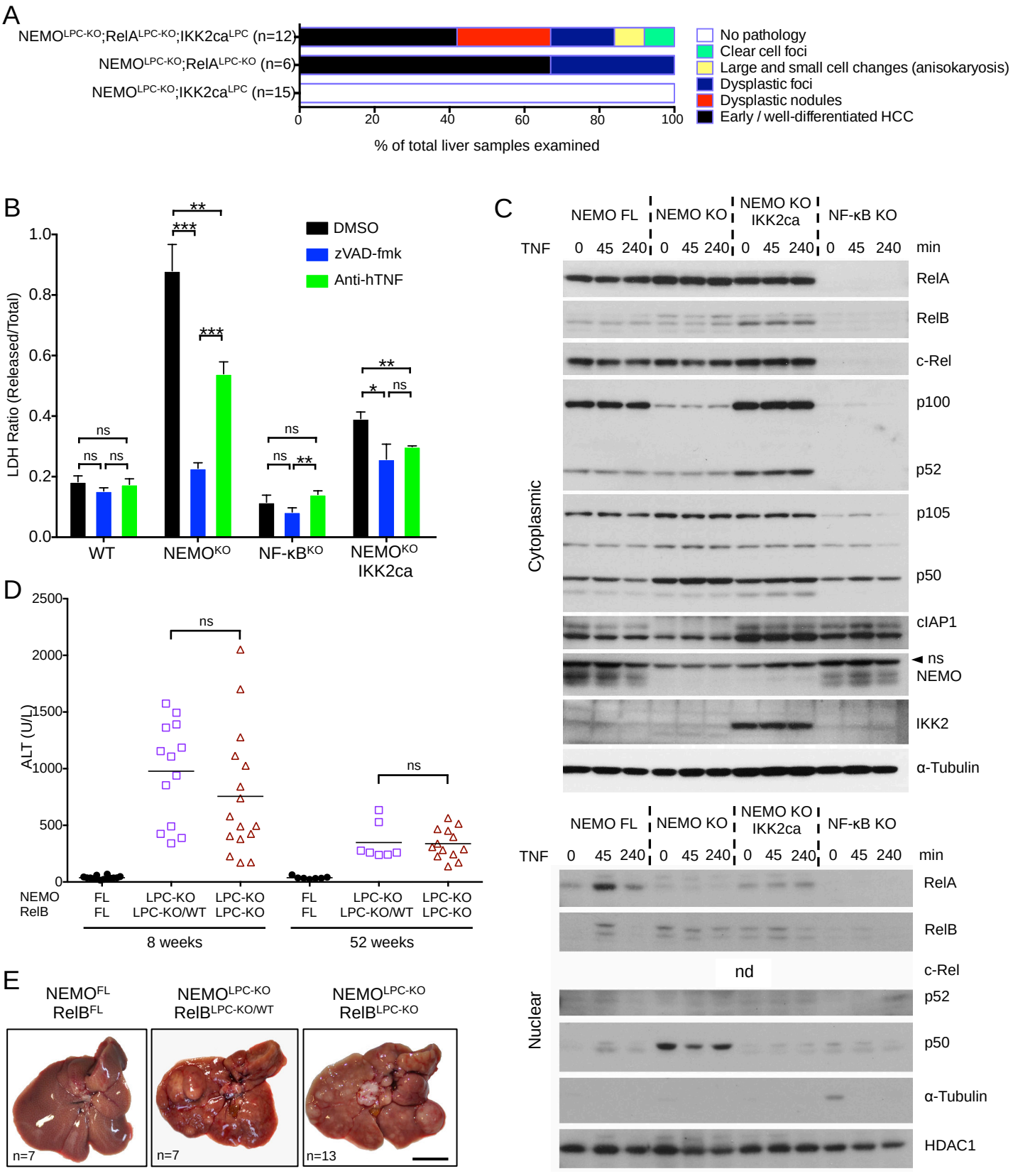
A
NEMO^LPC-KO;RelA^LPC-KO;IKK2ca^LPC (n=12)
NEMO^LPC-KO;RelA^LPC-KO (n=6)
NEMO^LPC-KO;IKK2ca^LPC (n=15)
0
20
40
60
80
100
% of total liver samples examined
No pathology
Clear cell foci
Large and small cell changes (anisokaryosis)
Dysplastic foci
Dysplastic nodules
Early / well-differentiated HCC
B
LDH Ratio (Released/Total)
1.0
0.8
0.6
0.4
0.2
0.0
DMSO
zVAD-fmk
Anti-hTNF
ns
**
***
*
WT
NEMO^KO
NF-κB^KO
NEMO^KO IKK2ca
C
NEMO FL
NEMO KO
NEMO KO IKK2ca
NF-κB KO
TNF
0 45 240 0 45 240 0 45 240 0 45 240 min
Cytoplasmic
RelA
RelB
c-Rel
p100
p52
p105
p50
cIAP1
ns
NEMO
IKK2
α-Tubulin
Nuclear
nd
HDAC1
D
ALT (U/L)
2500
2000
1500
1000
500
0
NEMO
RelB
FL
FL
LPC-KO
LPC-KO/WT
LPC-KO
LPC-KO
8 weeks
52 weeks
E
NEMO^FL RelB^FL
NEMO^LPC-KO RelB^LPC-KO/WT
NEMO^LPC-KO RelB^LPC-KO
n=7
n=7
n=13

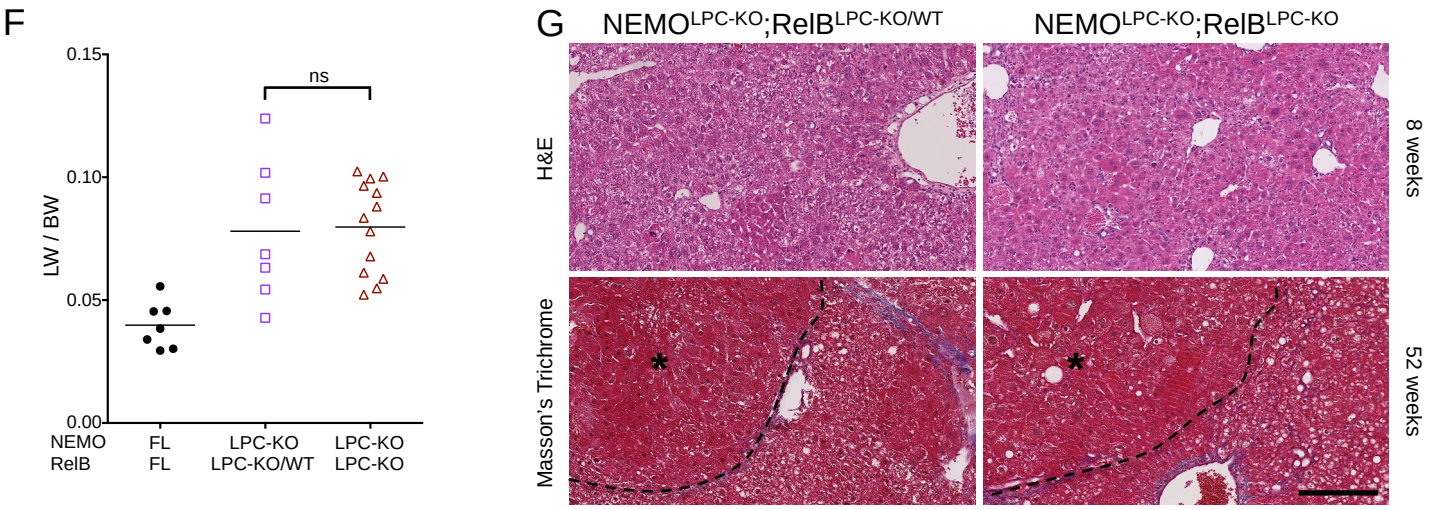

Figure S4, related to Figure 4: Non-canonical NF-κB signaling in hepatocytes is not involved in the liver pathology observed in NEMO^{LPC-KO} mice. (A) Histopathological evaluation of HCC development in one-year-old mice with the indicated genotypes. Each color bar represents the % of livers per genotype in which the indicated stage was identified as the most advanced disease stage. n is indicated. Four control floxed samples were examined without showing any pathological findings (not shown). (B) Spontaneous death of primary hepatocytes with the indicated genotypes after being cultured for 20 hr in the presence of DMSO (vehicle), zVAD-fmk or anti-hTNF antibody was estimated by measuring the released LDH-to-total LDH ratio. The results of a representative experiment are shown. Bars represent the mean ±SD (C) Primary hepatocytes with the indicated genotypes were cultured in the presence of zVAD-fmk and incubated with 20 ng/ml murine TNF for 45 or 240 min or left untreated followed by nuclear/cytoplasmic fractionation. Immunoblotting for the indicated proteins is shown. α-Tubulin was used as loading control for the cytoplasmic fraction and HDAC1 for the nuclear fraction. ns, non-specific band; nd, not detected. (D) Serum ALT levels in 8- and 52-week-old mice with the indicated genotype. Horizontal lines indicate mean values. (E) Representative liver images from 52-week-old mice with the indicated genotypes showing that NEMO^{LPC-KO};RelB^{LPC-KO} mice develop multiple liver tumors. (F) LW/BW ratios in 52-week-old mice with the indicated genotypes. Horizontal lines indicate mean values. (G) H&E and Masson's Trichrome staining in 8-week and 52-week-old mice, respectively. Scale bars: (E) 1 cm; (G) 200 μm.

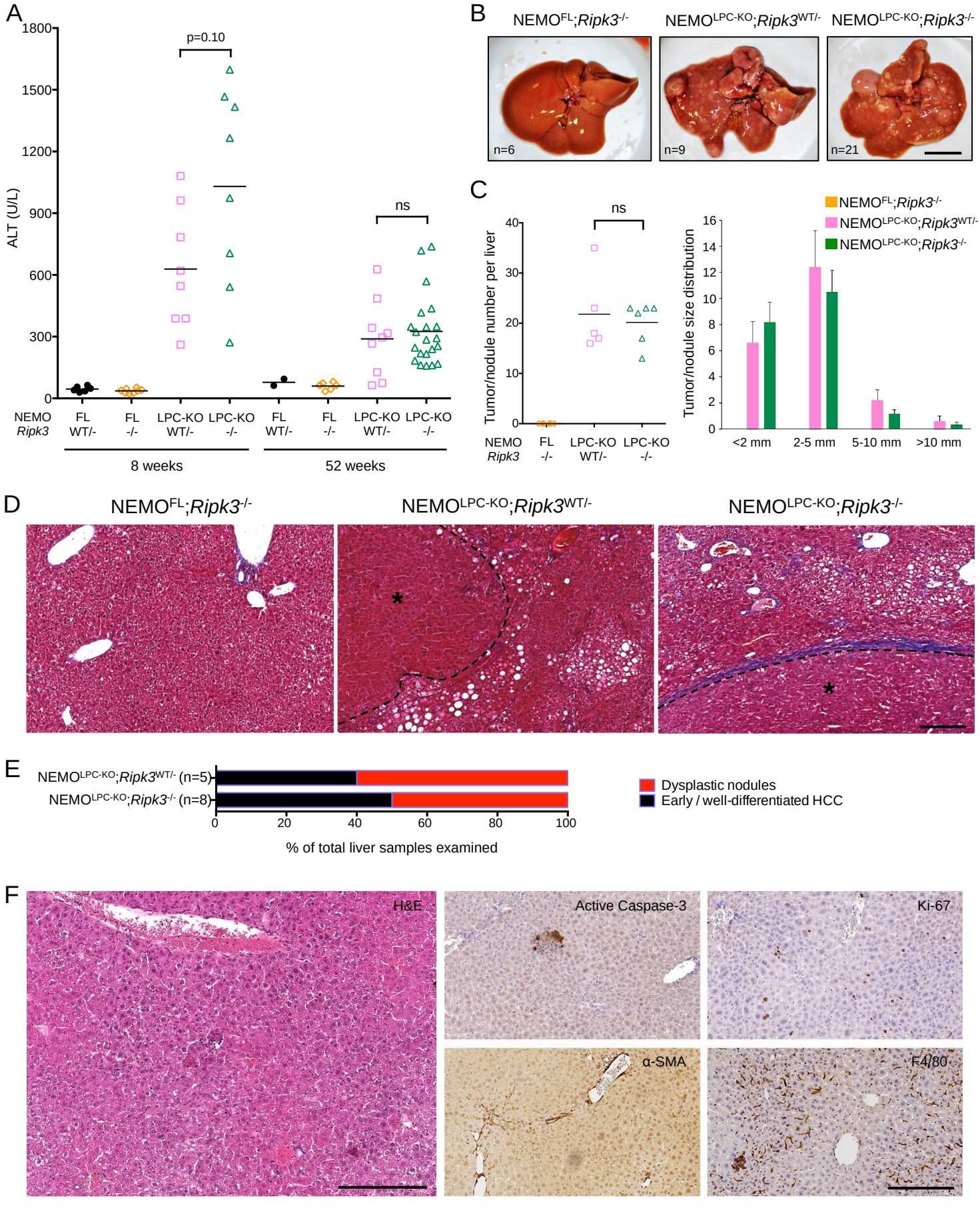
A
ALT (U/L)
1800
1500
1200
900
600
300
0
p=0.10
ns
NEMO
Ripk3
FL
WT/-
FL
-/-
LPC-KO
WT/-
LPC-KO
-/-
FL
WT/-
FL
-/-
LPC-KO
WT/-
LPC-KO
-/-
8 weeks
52 weeks
B
NEMOFL;Ripk3-/-
NEMOLPC-KO;Ripk3WT/-
NEMOLPC-KO;Ripk3-/-
n=6
n=9
n=21
C
Tumor/nodule number per liver
40
30
20
10
0
ns
NEMO
Ripk3
FL
-/-
LPC-KO
WT/-
LPC-KO
-/-
Tumor/nodule size distribution
16
14
12
10
8
6
4
2
0
NEMOFL;Ripk3-/-
NEMOLPC-KO;Ripk3WT/-
NEMOLPC-KO;Ripk3-/-
<2 mm
2-5 mm
5-10 mm
>10 mm
D
NEMOFL;Ripk3-/-
NEMOLPC-KO;Ripk3WT/-
NEMOLPC-KO;Ripk3-/-
*
*
E
NEMOLPC-KO;Ripk3WT/- (n=5)
NEMOLPC-KO;Ripk3-/- (n=8)
0
20
40
60
80
100
% of total liver samples examined
Dysplastic nodules
Early / well-differentiated HCC
F
H&E
Active Caspase-3
Ki-67
α-SMA
F4/80

Figure S5, related to Figure 5: RIPK3-deficiency does not prevent spontaneous hepatic damage and HCC in NEMO^{LPC-KO} mice. (A) Serum ALT levels in 8- and 52-week-old mice with the indicated genotype. Horizontal lines indicate mean values. (B) Representative liver images from 52-week-old mice with the indicated genotypes. (C) Assessment of tumor load in 52-week-old mice by estimating the average tumor number per liver and the tumor size distribution. Horizontal lines indicate the mean values. Bars represent mean ±SEM (n=8 mice per genotype). (D) Histological analysis of liver samples from 52-week-old mice by Masson´s trichrome staining. HCC areas are marked with an asterisk. (E) Histopathological evaluation of HCC development in one-year-old mice with the indicated genotypes. Each color bar represents the % of livers per genotype in which the indicated stage was identified as the most advanced disease stage. n is indicated. Three control liver samples from *Ripk3*$^{-/-}$ mice were examined without exhibiting any pathological findings (not shown). (F) H&E staining and immunohistochemistry for active caspase-3, Ki-67, α-SMA and F4/80 were performed on liver sections from 8-week-old mice RIPK1^{LPC-KO}. Scale bars: (B) 1 cm; (D, F) 200 µm.

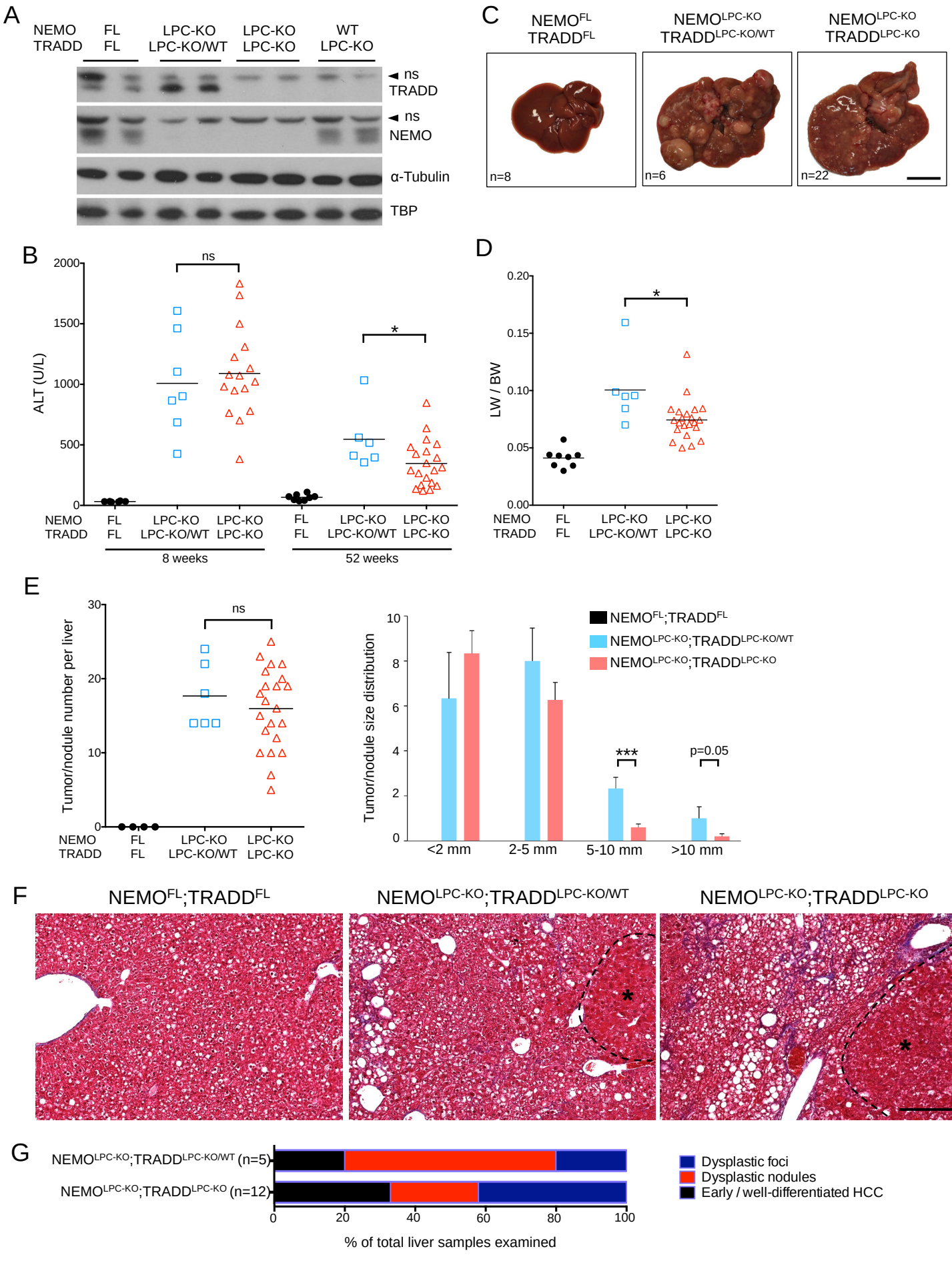
A
NEMO
TRADD
FL
FL
LPC-KO
LPC-KO/WT
LPC-KO
LPC-KO
WT
LPC-KO
ns
TRADD
ns
NEMO
α-Tubulin
TBP
C
NEMO^FL
TRADD^FL
NEMO^LPC-KO
TRADD^LPC-KO/WT
NEMO^LPC-KO
TRADD^LPC-KO
n=8
n=6
n=22
B
ALT (U/L)
2000
1500
1000
500
0
ns
*
8 weeks
52 weeks
D
LW / BW
0.20
0.15
0.10
0.05
0.00
*
E
Tumor/nodule number per liver
30
20
10
0
ns
Tumor/nodule size distribution
10
8
6
4
2
0
NEMO^FL;TRADD^FL
NEMO^LPC-KO;TRADD^LPC-KO/WT
NEMO^LPC-KO;TRADD^LPC-KO
***
p=0.05
<2 mm
2-5 mm
5-10 mm
>10 mm
F
NEMO^FL;TRADD^FL
NEMO^LPC-KO;TRADD^LPC-KO/WT
NEMO^LPC-KO;TRADD^LPC-KO
G
NEMO^LPC-KO;TRADD^LPC-KO/WT (n=5)
NEMO^LPC-KO;TRADD^LPC-KO (n=12)
0
20
40
60
80
100
% of total liver samples examined
Dysplastic foci
Dysplastic nodules
Early / well-differentiated HCC

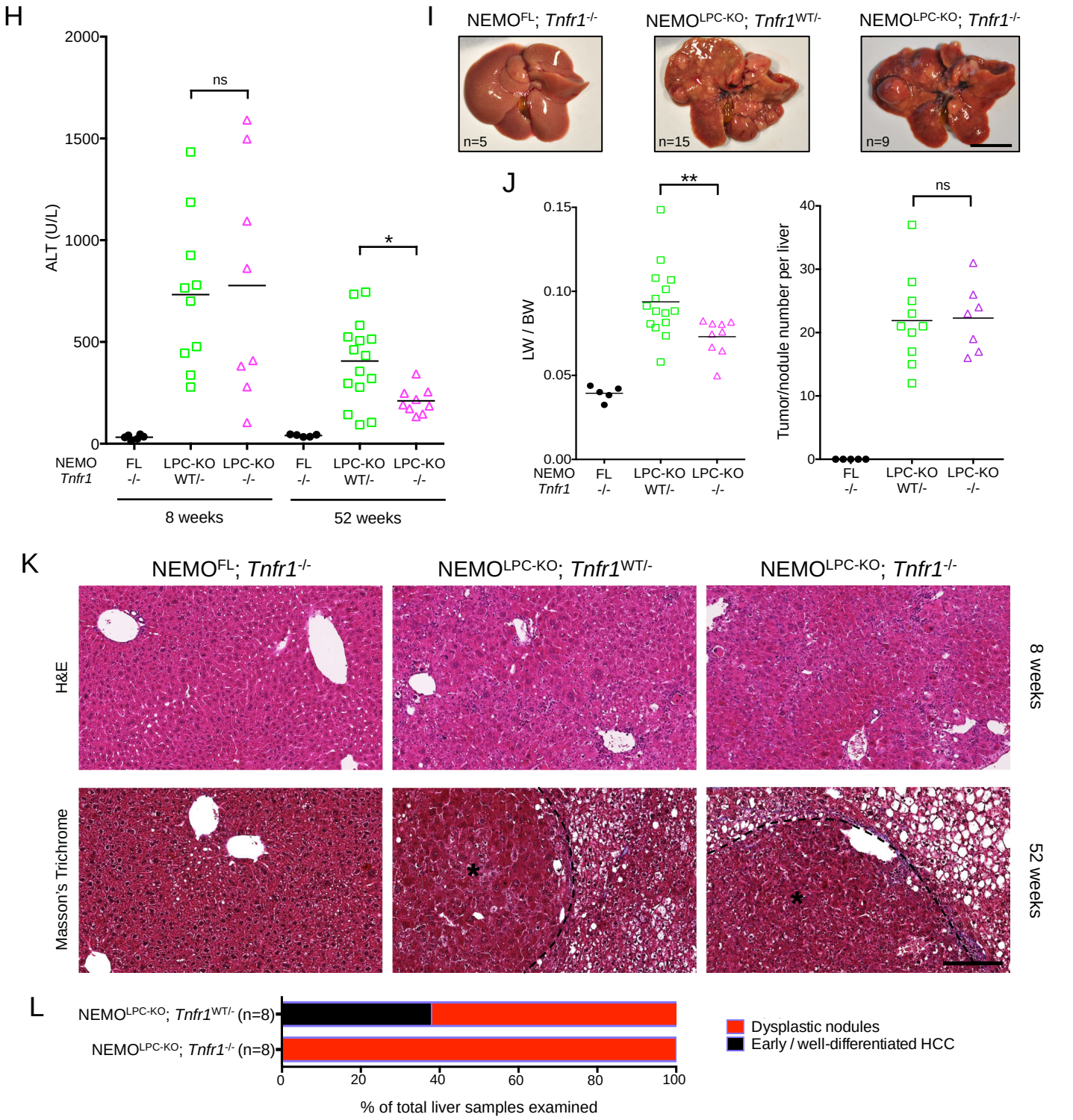

Figure S6, related to Figure 7: LPC-specific TRADD deficiency or whole-body TNFR1 deficiency do not prevent hepatocyte death and HCC development in NEMO^{LPC-KO} mice. (A) Deletion efficiency of TRADD and NEMO in liver lysates from 52-week-old mice with the indicated genotypes as assessed by immunoblotting. α-Tubulin and TBP were used as loading controls. (B) Serum ALT levels in 8- and 52-week-old mice with the indicated genotype. (C) Representative liver images from 52-week-old mice with the indicated genotypes. (D-E) Tumor load in mice with the indicated genotypes was estimated by quantification of the LW/BW ratios (D) and the average tumor number per liver and tumor size distribution (E). Bars represent mean ±SEM (n=6 for NEMO^{LPC-KO};TRADD$^{LPC-KO/WT}$ mice and n=21 for NEMO^{LPC-KO};TRADD^{LPC-KO} mice). (F) Histological examination of liver samples from 52-week-old mice by Masson´s trichrome staining. HCC/dysplastic nodules are marked with an asterisk. (G) Histopathological evaluation of

HCC development in one-year-old mice with the indicated genotypes. Three floxed control samples were examined without showing any pathological findings (not shown). (H) Serum ALT levels in 8- and 52-week-old mice with the indicated genotype. (I) Representative liver images from 52-week-old mice with the indicated genotypes. (J) Tumor load in mice with the indicated genotypes was estimated by quantification of the LW/BW ratios and the average tumor number per liver. (K) Histological examination of liver samples from 8- and 52-week-old mice with the indicated genotypes after H&E and Masson´s trichrome staining, respectively. HCC areas are marked with an asterisk. (L) Histopathological evaluation of HCC development in one-year-old mice with the indicated genotypes. Three *Tnfr1*$^{-/-}$ control samples were examined without showing any pathological findings (not shown). Horizontal lines in B, D, E, H and J indicate mean values. Each color bar in G and L represents the % of livers per genotype in which the indicated stage was identified as the most advanced disease stage (n is indicated). Scale bars: (C, I) 1 cm; (F, K) 200 µm.

Supplemental Experimental Procedures

Histology, Immunohistochemistry (IHC) and quantification

Tissues were fixed overnight in 4% paraformaldehyde, embedded in paraffin, and cut into 5 µm sections. H&E-stained sections were examined in a blind fashion for the amount of inflammation, tissue damage, and tumorigenesis. Collagen was visualized using Masson's Trichrome stain kit (Sigma-Aldrich, HT15-1KT) according to manufacturer's instructions.

For IHC staining, paraffin sections were rehydrated and antigen retrieval was performed either by heating in 10 mM sodium citrate, 0.05% Tween-20 at pH 6.2 or by incubation with 20 µg/ml proteinase K (Roche). The following antibodies were used: anti-Ki67 (DAKO, M724901), anti-active caspase-3 (R&D Systems, AF835), α-SMA (Sigma-Aldrich, A2547), anti-F4/80 (AbD Serotec, clone A3-1), anti-Gr1/Ly6G (BD Biosciences, 551459), anti-B220 (clone RA3 6B2, homemade), anti-CD3 (Abcam, ab5690), anti-RelA (Santa Cruz, sc-372), CK19 (Developmental Studies Hybridoma Bank, TROMA-III). Biotinylated secondary antibodies were purchased from Perkin Elmer, DAKO and Vector Laboratories. Stainings were visualized with ABC Kit Vectastain Elite (Vector Laboratories) and DAB substrate (DAKO). For optimal visualization, levels and brightness/contrast adjustments of the pictures were equally applied using Adobe Photoshop.

IHC quantification was performed on 3 randomly selected high power fields (HPF) per liver section. Liver sections from 3-5 mice per genotype were analyzed. Quantification of Ki-67$^+$ and active Caspase-3$^+$ apoptotic hepatocytes, Gr1/Ly6G$^+$ granulocytes, CD3$^+$ T cells and B220$^+$ B cells was performed manually. α-SMA$^+$ activated hepatic stellate cells and F4/80$^+$ macrophages were quantified using Image J software (Version 1.48; http://rsbweb.nih.gov/ij/) by applying the appropriate pixel threshold equally on all selected pictures and using measure function to calculate the covered area. Data is represented as % of covered area for each cell type over total tissue area.

Histopathological evaluation of HCC development in one-year-old mice

H&E stained liver sections from mice were assessed for the presence and the stage of HCC development in the following ascending order of severity: No pathology, clear cell foci, small and large cell changes (anisokaryosis), dysplastic foci, dysplastic nodules and early or well-differentiated HCC. Each liver sample was placed in the most advanced hepatocarcinogenesis stage, despite the fact that areas with characteristics of less advanced stages were also observed in these samples. In the corresponding graphs, each bar represents the % of livers per genotype in which the indicated stage was identified as the most advanced disease stage.

Quantitative RT–PCR

Total RNA was extracted from primary hepatocytes using NucleoSpin® RNA II Total RNA isolation Kit (Macherey-Nagel) following the manufacturer's protocol and cDNA was prepared with Superscript III cDNA-synthesis Kit (Life Technologies). qRT–PCR was performed with TaqMan probes (Life Technologies) using TATA-box-binding protein (TBP) as a reference gene. Relative expression of gene transcripts was assessed by using the 2-ΔΔCt method. Primer sequences are available upon request.

Hepatocyte isolation

Primary hepatocytes were isolated from ~ 4-week-old mice as described previously (Ehlken et al., 2011). In brief, anesthetized mice were perfused via the vena cava with solution I (EBSS without Ca^{2+} and Mg^{2+}, 0,5 mM EGTA). Subsequently, perfusion with 50 ml of collagenase solution (EBSS with Ca^{2+} and Mg^{2+}, 10 mM HEPES, 3810 U collagenase and 2 mg Trypsin inhibitor) was performed and single cell suspensions of perfused liver were generated using a 70 µm nylon mesh. Hepatocytes were washed twice in high glucose DMEM supplemented with 2% FCS, penicillin and streptomycin, followed by seeding on collagen-coated plates. The medium was renewed 4 hr later to remove any unattached/dying cells.

Cell Death assays

Death of primary hepatocytes in vitro was estimated using an LDH release-based cytotoxicity assay (Promega) after incubating primary hepatocytes for 20 hr in the absence or presence of 20 µM zVAD-fmk (Enzo LifeSciences) or 1 mg/ml hTNFR2:Fc (Etanercept). LDH ratio (released vs. total LDH) was estimated on samples of cell supernatant before and after cell lysis with 1% Triton X-100 using CytoTox 96 cytotoxicity assay (Promega) according to the manufacturer's protocol. The results were normalized to the average value of vehicle-treated hepatocytes that was set as 100%. The experiments were performed in triplicates using primary hepatocytes that were isolated from at least 3 different mice per indicated genotype.

Immunoprecipitation (IP) and Immunoblotting

Primary hepatocytes isolated from mice with the indicated genotypes were cultured for 20 hr in the presence of 20 µM zVAD-fmk, and then were lysed in 20 mM HEPES-KOH pH 7.6, 150 mM NaCl, 1.5 mM $MgCl_2$, 1 mM EGTA, 1% Triton X-100, 10% glycerol, phosSTOP phosphatase inhibitors (Roche) and complete protease inhibitors (Roche). RIPK1 and FADD were immunoprecipitated from the soluble lysates by overnight incubation at 4°C using a rat anti-RIPK1 antibody (rat clone 10C7.3.1, kindly provided by Genentech) or a goat anti-FADD antibody (Santa Cruz, sc-6036) coupled to protein G Dynabeads (Life Technologies). Beads were washed extensively in cold lysis buffer and then eluted by heating in SDS-containing sample buffer.

Protein extracts from primary hepatocytes or whole liver samples were prepared in high-salt RIPA buffer (20 mM HEPES, pH 7.6; 350 mM NaCl; 20% glycerol; 1 mM $MgCl_2$; 0.5 mM EDTA; 0.1 mM EGTA; 1% NP-40) supplemented with phosSTOP phosphatase inhibitors (Roche) and complete protease inhibitors (Roche).

Lysates were separated by SDS-polyacrylamide gel electrophoresis (PAGE), transferred to Immobilon-P PVDF membranes (Millipore), and analyzed by immunoblotting. Membranes were probed with primary antibodies against following proteins: NEMO (home made (Luedde et al., 2007)), RelA (Santa Cruz, sc-372), c-Rel (Santa Cruz, sc-71), RelB (Santa Cruz, sc-226), p100/p52 (NR1495), p105/p50 (Santa Cruz, sc-114), IKK2 (Cell Signaling, #2684), RIPK1 (610459, BD Biosciences and Genentech rat clone 10C7.3.1), FADD (Millipore, 50-171-656), Caspase-8 (Enzo LifeSciences; ALX-804-447), TRADD (Santa Cruz, sc-7868), RIPK3 (Enzo LifeSciences; ADI-905-242), cFLIP (Enzo LifeSciences; AG-20B-0005), cIAP1 (Enzo LifeSciences; ALX-803-335), TRAF2 (Santa Cruz, sc-876), TRAF3 (Santa Cruz, sc-947), JNK (Cell Signaling, #9252), Phospho-JNK (Cell Signaling, #9251), cleaved caspase-3 (Cell Signaling, #9661), caspase 3 (Cell Signaling, #9662), HDAC1 (Santa Cruz, sc-7872), actin (Santa Cruz, sc-1616), α-tubulin (Sigma-Aldrich, T6074), GAPDH (IMG-5019A-1, Imgenex). Membranes were then incubated either with secondary HRP-coupled antibodies (GE Healthcare and Jackson ImmunoResearch) and developed with chemiluminescent detection substrate (GE Healthcare) or with secondary antibodies coupled to IRDye680 or 800 and visualized with Odyssey infrared imaging system (Licor). Band quantification was performed using ImageJ.

Subcellular fractionation

Primary hepatocytes were treated with 20 ng/ml murine TNF for 45 min or 4 hr or left untreated. The cells were directly lysed in hypotonic buffer (50 mM Tris-HCl pH 8.0, 2 mM EDTA, 10% glycerol and 0.1% Nonidet P-40) for 10 min on ice, followed by centrifugation for 5 min at 2300 × *g* at 4 °C. The supernatants were collected as cytoplasmic extracts. The pellets were washed twice with hypotonic buffer and lysed with high-salt buffer (see IP buffer). Cell lysates were centrifuged for 10 min at 16,000 × *g* at 4°C, and the supernatants were collected as nuclear extracts.

Supplemental References

Ehlken, H., Kondylis, V., Heinrichsdorff, J., Ochoa-Callejero, L., Roskams, T., and Pasparakis, M. (2011). Hepatocyte IKK2 protects Mdr2-/- mice from chronic liver failure. PloS one *6*, e25942.